THE AMERICAN SOCIETY OF MECHANICAL ENGINEERS
345 E. 47th St., New York, N.Y. 10017

94-GT-389

OBSERVATIONS OF FLAME BEHAVIOR FROM A PRACTICAL FUEL INJECTOR USING GASEOUS FUEL IN A TECHNOLOGY COMBUSTOR

Paul O. Hedman
Dept. of Chemical Engineering
Advanced Combustion
Eng. Research Center
Brigham Young Univ.
Provo, Utah

Geoffrey J. Sturgess
Pratt & Whitney Aircraft Co.
East Hartford, Connecticut

David L. Warren
Dept. of Mechanical Eng.
Advanced Combustion
Eng. Research Center
Brigham Young Univ.
Provo, Utah

Larry P. Goss
Systems Research Laboratories, Inc.
A Division of Arvin/Calspan
Dayton, Ohio

Dale T. Shouse
Wright Laboratory
Wright-Patterson AFB, Ohio

ABSTRACT

This paper presents results from an Air Force program being conducted by researchers at Brigham Young University (BYU) Wright-Patterson Air Force Base (WPAFB), and Pratt and Whitney Aircraft Co (P&W). This study is part of a comprehensive effort being supported by the Aero Propulsion and Power Laboratory at Wright- Patterson Air Force Base, and Pratt and Whitney Aircraft, Inc. in which simple and complex diffusion flames are being studied to better understand the fundamentals of gas turbine combustion near lean blowout. The program's long term goal is to improve the design methodology of gas turbine combustors.

This paper focuses on four areas of investigation: 1) digitized images from still film photographs to document the observed flame structures as fuel equivalence ratio was varied, 2) sets of LDA data to quantify the velocity flow fields existing in the burner, 3) CARS measurements of gas temperature to determine the temperature field in the combustion zone, and to evaluate the magnitude of peak temperature, and 4) two-dimensional images of OH radical concentrations using PLIF to document the instantaneous location of the flame reaction zones.

INTRODUCTION

As part of a comprehensive Air Force program, three different combustors have been utilized to investigate lean blowout in aircraft gas turbine engines. These vehicles consist of a simplified research combustor (Task 100), a technology combustor (Task 150), and a simplified, generic gas turbine combustor (Task 200). The technology combustor (Task 150) incorporates the practical fuel injectors used in the generic gas turbine combustor (Task 200) into the simpler research combustor (Task 100), to permit study of injector characteristics in isolation. The work presented concerns work with the Task 150 technology combustor. While many detailed studies exist in the literature concerning jet flames, both free and enclosed, almost nothing is available on the flame characteristics produced by practical ways of introducing the reactants into an engine combustor. This work goes some way towards remedying this situation.

The Task 150 technology combustor uses a practical liquid fuel injector with a classic gas turbine engine air blast atomizing configuration, involving co-swirling airsheets on either side of a co-swirling annular (normally liquid) fuel sheet, with the outer air passage and the fuel passage both converging on the central air passage. For this study, the burner was fueled by gaseous propane. Two injectors of this same configuration have been used, high-swirl (HS) and low-swirl (LS) injectors. Only data from the high-swirl configuration are reported in this paper. The technology combustor has been configured so that the geometry around the injector is nearly axi-symmetric with a diameter of about 150 mm. However, the combustor incorporates flat quartz windows about 60 mm in width on each of four sides so that laser based optical diagnostic instruments can be used. This unique configuration allows complex diagnostic measurements to be made in a simpler geometry than the Task 200 generic gas turbine combustor, but which embodies most of the features of an actual jet engine combustor in a near axi-symmetric configuration that is easier to mathematically model. Four methods of measurements have been used to characterize the flame. These include still film photographs, LDA measurements of velocity, CARS measurements of gas temperature, and images from PLIF measurements of the OH radical.

Experimental tests have been conducted on the research combustor at both BYU and WPAFB locations. These tests included operational characteristics, flow partitioning in various injector passages, visual flame structure, planner laser induced fluorescence (PLIF) imaging of OH radicals in the flame boundary, laser Doppler anemometry (LDA) velocity information, and coherent anti-Stokes Raman spectroscopy (CARS) temperature data. The effects of various parameters on the fuel equivalence ratio at lean blowout (LBO), an important operational characteristic, have also been investigated but are not reported in this paper.

Presented at the International Gas Turbine and Aeroengine Congress and Exposition
The Hague, Netherlands — June 13–16, 1994
This paper has been accepted for publication in the Transactions of the ASME
Discussion of it will be accepted at ASME Headquarters until September 30, 1994

Intriguing flame structures have been visually observed, and captured in video images, digitized still photographs, and PLIF images of the OH radical with the Task 150 configuration. The digitized images from still photographs have characterized the flame shapes observed visually. The instantaneous two-dimensional PLIF images have frozen flame structures missed with the visual observations. The partitioning of air flows through the dome and insert jets, and the primary and the secondary air swirlers was also determined. Preliminary analysis of PLIF images of the OH radical, combined with air flow split information, have helped describe the basic mixing patterns observed as the fuel equivalence ratio is changed. The flame attaches to the burner or lifts from the burner as the fuel equivalence ratio is changed.

LDA measurements have quantified the axial, radial, and tangential velocity components in the combustor for two operating conditions ($\phi = 0.72$ and $\phi = 1.49$) at an air flow rate of 500 slpm. This information has yielded local velocity and turbulence data and preliminary analysis of zero axial velocity contours has been used to identify the major recirculation zones. Data from both isothermal flows and combusting hot flows have been collected. Mean axial, tangential, and radial velocity LDA data for combusting hot flow data are presented in the paper. This data is also useful for model validation.

CARS gas temperature data have also been collected for the Task 150 technology combustor with the high swirl injector at an air flow rate of 500 slpm and at fuel equivalence ratios (ϕ) of 0.75, 1.00, 1.25, and 1.50. This unique set of data shows the corresponding geometrical changes in the structure of the mean gas temperature distribution as fuel equivalence ratio is changed, and quantifies the change in the magnitude of the peak temperature as the fuel equivalence ratio changes from lean, to stoichiometric, to fuel rich. Mean gas temperature data for $\phi = 0.75$, 1.00, and 1.50 are presented in the paper.

COMBUSTOR TEST FACILITY

Three burners are being utilized as part of a comprehensive Air Force program to investigate lean blowout in the combustors of aircraft gas turbine engines (Sturgess, et al., 1991b). These vehicles consist of the simplified Task 100 research combustor, the Task 150 technology combustor, and the Task 200 simplified, generic gas turbine combustor. This work provides a bridge between the combustion characteristics of confined, coannular fuel and air jets discharged into a sudden expansion (Task 100 research combustor) and the characteristics of a linear array of four swirling fuel injectors installed in a rectangular combustion chamber that simulates a segment of a real jet engine combustor (Task 200 simplified, generic gas turbine combustor). The Task 150 technology combustor incorporates one of the practical fuel injectors used in the Task 200 generic gas turbine combustor into the simpler Task 100 research combustor, to permit study of its characteristics in isolation. The use of the Task 150 technology combustor allows the combustion characteristics of a real injector to be investigated in a simple geometry where various diagnostic measurements (primarily laser-based optical measurements) can be more easily made.

In an actual engine combustor, additional combustion and cooling air is added to the combustor downstream of the actual fuel injector. This adds an additional complexity to the flow and combustion characteristics which is being investigated in a subsequent study. Only the characteristics in the zone near the injector are presented in this paper.

The work reported herein was accomplished in identical burners available in the Combustion Laboratories at BYU and WPAFB respectively. The burners were designed by researchers at P&W (Sturgess, et al., 1992a) and fabricated at WPAFB. The features of the dome and injector can be seen in Figure 1. The type injector used in this study is a classic gas turbine engine air blast atomizing configuration, involving co-swirling airsheets on either side of a co-swirling annular (normally liquid) fuel sheet, with the outer air passage and the fuel passage both converging on the central air passage.

Two injectors of this same configuration were used. The high-swirl (HS) injector has a nominal swirl number (based on vane angle) of 1.41, and the low-swirl (LS) injector has a nominal swirl number of 1.05. The total air passage effective areas were 0.176 in^2 for the HS injector and 0.266 in^2 for the LS injector, with outer to inner flow splits of 2.8 and 2.2 respectively. The outer swirler vane angle was 55 degrees for both injectors, while the inner swirler vane angle was 70 degrees for the HS injector and 45 degrees for the LS injector. The injectors were mounted in a plain bulkhead dome containing insert jets angled at 12.5 degrees into the flame, and radially outwards flowing film cooling jets. This arrangement closely simulates that of an engine combustor. The total effective air flow area of the dome, excluding the fuel injector, was 0.160 in^2.

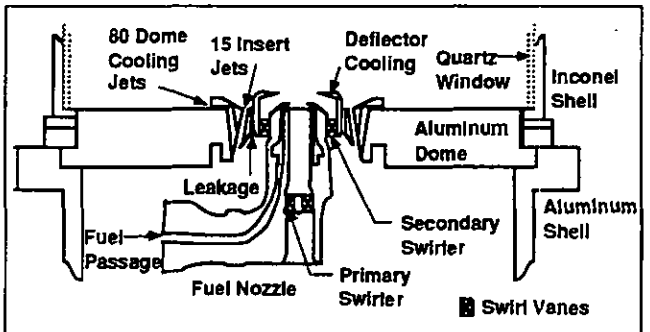

FIGURE 1. SCHEMATIC OF THE T150 HIGH SWIRL INJECTOR

The combustion chamber, shown in Figure 2, has been designed to be nearly axisymmetric and incorporate quartz windows to allow optical diagnostics (primarily laser-based optical measurements) to be made. The combustor cross-section is square with generously filleted corners to minimize secondary flow development. The hydraulic diameter is 150 mm. This box-section combustor with corner fillets allows reasonable optical access while providing a cross section that approximates a two-dimensional axisymmetric cross section. The bluff body provides a recirculation region which can stabilize the flame. Optical windows of fused quartz are provided on the four flat sides for a downstream length of 490 mm. The combustor overall length to hydraulic diameter ratio is 4.9, and the exit blockage is 45 percent by means of an orifice plate. The only air addition in this configuration is through the dome.

The combustor is mounted on a 240 mm length spool piece containing a mounting pad for the fuel injector flange. The combustor and spool piece are situated on an inlet air conditioning section, also shown in Figure 2. Reactants are supplied at ambient temperature and pressure. Ignition is by means of a removable torch-ignitor. This combustion chamber allows the combustion characteristics of a practical injector to be investigated in a simple geometry where various diagnostic measurements can be made.

In order to separate the effects of liquid fuel atomization and spray droplet evaporation from the effects associated with fuel/air mixing and aerodynamic flow pattern, these first evaluations involved the use of a gaseous propane fuel. Planned subsequent evaluations will use liquid ethanol. Liquid ethanol is expected to closely simulate the combustion characteristics of the liquid jet fuels, but without significant soot formation. Extensive sooting could cloud the quartz windows precluding easy optical access. The present paper deals exclusively with propane results with the HS injector.

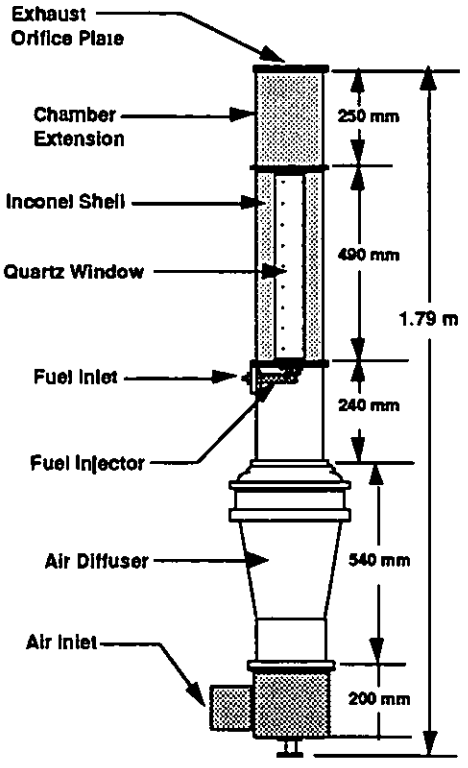

FIGURE 2. LABORATORY-SCALE GAS TURBINE COMBUSTOR

The results presented concern work with the Task 150 technology combustor using the high-swirl injector and gaseous propane fuel. While many detailed studies exist in the literature concerning jet flames, both free and enclosed, almost nothing is available on the flame characteristics produced by practical ways of introducing the reactants into an engine combustor. This work goes some way towards remedying this situation.

PHOTOGRAPHIC FLAME CHARACTERIZATION

A complex series of intricate flame structures have been observed in the Task 150 technology combustor according to the operating conditions and fuel injector used. Some of the flame behavior could be related to that seen in the Task 100 research combustor (Sturgess et al., 1991a; Sturgess et al., 1992b), and some of the structures to those seen in the Task 200 generic combustor (Sturgess and Shouse, 1993). These flame structures were studied directly with use of visual observations, video recordings, and still photography. The still film photographs have been digitized and filtered using computer techniques to produce isochromatic contour plots, Figure 3, for quantitative purposes.

One of the traits of the Task 150 technology combustor is the wide variety of flame structures that are observed. Each flame shape indicates a different mode of operation, which differ from one another in the location of the flame fronts, or by some structure such as thickness or intensity. The different structures observed arise from changes in the flow fields, mixing patterns, or fuel equivalence ratio as operating conditions are varied. The differences and similarities of the flame structures for the swirling injectors together with the results from the co-axial jet diffusion flame (Task 100 combustor) provide significant insights to the combustion processes. The shape of the flame, at the minimum, provides qualitative information on the mixing process and location of flame fronts. Such information can yield insights into the processes present. Flames fronts exist because fuel and oxidizer have been transported to a point where combustion can be supported. The location of these fronts relative to the outlet orifices of fuel and air are of obvious interest.

The fuel equivalence ratios where the transitions from one flame structure to another were determined as a function of fuel flow rate. The flames for both Task 150 injectors were attached to the outside of the insert air jets when the burner was operated very fuel rich. The flame would then lift, reattach, and lift again as the fuel equivalence ratio was progressively reduced depending on the injector (high swirl versus low swirl) and the air flow rate. During the reattachment phase, the flame would take on many of the characteristics of a strong vortex, and shared many features associated with a tornado. Consequently, the terminology of funnel cloud, tornado, and debris cloud were adopted to differentiate some of the observed flame structure from the general description of a vortex flow.

The characterization of the flame structure was carried out by visual observations. Still film photographs were taken of the different structures. These images were digitized and manipulated using various computer programs into the isochromatic contour plots found in Figure 3 for the high swirl injector. The major factor affecting in flame structure was the overall fuel equivalence ratio in the burner determined from total air and fuel flow rates, and to a much lesser extent the air flow rate. At a given air flow rate, the fuel would be reduced until a transition in flame structure was judged to have been reached. These observations were not easily made. With the high swirl nozzle, the flame structures flowed smoothly from one mode to another. These smooth transitions left no sharp break point in flame behavior. Consequently, the images presented in Figure 3 are only representative of the types of flame structures observed.

At very fuel rich conditions (ϕ = 2.38 and ϕ = 1.72), the flame was attached to the insert jets, in a manner similar to

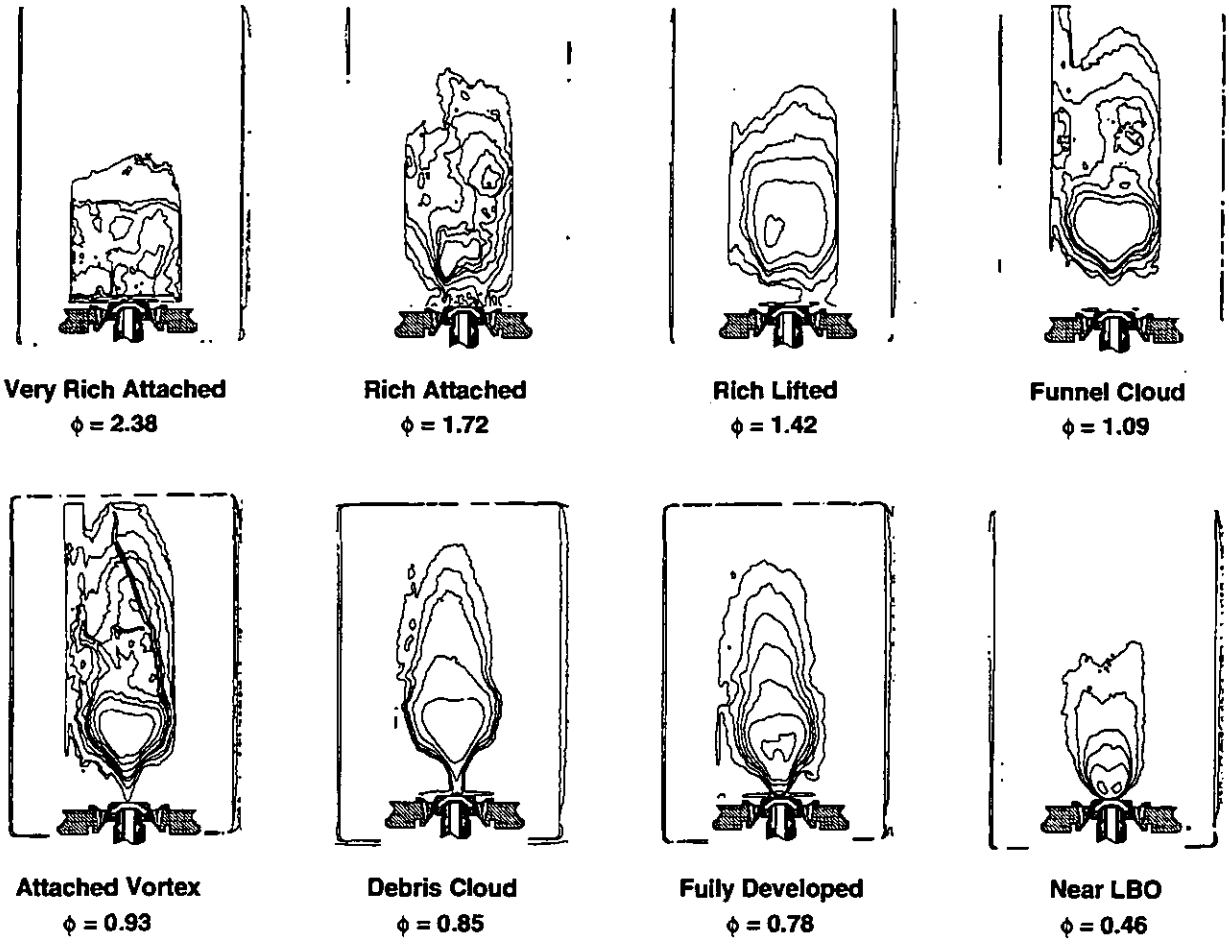

FIGURE 3. CHARACTERISTIC FLAME SHAPES FROM DIGITIZED STILL PHOTOGRAPHS (T150-HS NOZZLE, 310 SLPM AIR)

that observed with the Task 100 technology combustor at rich conditions. Unlike the Task 100, however, these flames were very short, presumably because of the much faster mixing due to the swirling motion of the gases. As the amount of fuel was further reduced (decreasing fuel equivalence ratio at a constant air flow rate), the still rich flame lifted and stabilized on a downstream recirculation zone that appeared to be associated with the injector ($\phi = 1.42$). The primary combustion zone continued to lengthen as relatively less fuel entered the combustion chamber ($\phi = 1.42$ to $\phi = 1.09$).

After the rich lifted condition, further reductions in fuel equivalence ratio caused the flame to stabilize in the rapidly swirling vortex at the center of the combustor, with flame structures that resembled the development of a tornado. As seen in Figure 3, a structure that resembled a funnel cloud formed within the rich lifted flame ($\phi = 1.09$) and gradually descended as the fuel flow was continually decreased ($\phi = 1.09$ to $\phi = 0.93$) forming a tornado like flame structure. Further reductions in ϕ caused the tornado like flame to enter the primary swirler passage in the injector ($\phi = 0.93$). Continued reduction in fuel equivalence ratio caused a flame in the shape of a bowl, which looked much like the debris cloud of a tornado, to attach to the nozzle on the outside of the tornado like structure ($\phi = 0.85$). The minute detail of the debris cloud was lost in the process of converting from the still photograph to the image presented in Figure 3. Continued reduction of the fuel flow resulted in the growth in size and intensity of the debris cloud like flame structure while the funnel cloud like structure was simultaneously decreasing. The total disappearance of the funnel cloud structure marked a transition to a fully developed flame that was strongly attached to the center of the injector ($\phi = 0.78$). At lower air flow rates (less than ca 500 slpm), this strongly attached flame would weaken until the lean blowout limit ($\phi = 0.46$) was reached (blowout occurred from an attached flame). At high air flow rates (greater that ca 500 slpm), the flame would once again lift, attach to a down stream recirculation zone, and eventually

blowout from the separated flame structure ($\phi = 0.42$), much like that observed in the Task 100 research combustor.

GAS VELOCITY MEASUREMENTS

A laser Doppler anemometer (LDA) was used to make extensive measurements of gas velocity in the burner at five separate experimental conditions. The experimental conditions used are summarized in Table 1.

TABLE 1
SUMMARY OF EXPERIMENTAL CONDITIONS FOR LDA MEASUREMENTS

Injector	Flow	Air slpm (70 F)	C_3H_8 slpm (0 C)	N_2 slpm (0 C)	ϕ
T150HS	Cold	500		14	0.72
T150HS	Hot	500	14		0.72
T150HS	Cold	500		29	1.49
T150HS	Hot	500	29		1.49
T100	Cold	1000		23	0.59

The LDA measurements reported in this paper are for the Task 150 burner with the high swirl injector installed. Measurements were made for lean conditions ($\phi = 0.72$) where the flame was well attached to the central part of the injector, and also at fuel rich conditions ($\phi = 1.49$) where the flame was attached to the dome and insert jets. LDA measurements were also obtained in isothermal, non-reactive flows where nitrogen was substituted for the propane fuel. This has allowed the effect of the flame temperature on the flow field and gas velocities to be determined for at least two of the test conditions used. However, only the data from the combusting flow experiments are reported in this paper.

A schematic of the LDA experimental set-up is presented in Figure 4. The beam from the argon-ion laser was split into two beams, frequency shifted (40 and 34 MHz), polarized, and focused into a diagnostic volume in the test section. The forward-scattered LDA signals for the radial (or tangential) and axial velocity components were focused into fiber optic cables and passed to a photo multiplier tube to be amplified and converted to electrical signals. These electrical signals were collected with TSI, Inc. counters and analyzed with a Macintosh IIfx computer. A Le Croy 9314L Quad 300 MHz oscilloscope was used to monitor the Doppler bursts to help in the alignment of the LDA system and to insure quality data was being collected. Even with careful alignment, there was still some noise which was filtered using a data analysis program.

A brief investigation was made to evaluate the effect of the number of points taken at a given test location on the accuracy of the gas velocity measurement. Three different sets of data were collected, a set with 5000 points, a set with 2000 points,and a set with 1000 points. In general, there was little difference observed in the mean axial and tangential velocities determined from the different number of points in the data sets. However, the fluctuating velocity components (i.e. rms velocities) were better described by the data sets containing the largest number of points. Nevertheless, for this study, 1000 data points were collected at each test location. This allowed a greater number of experimental conditions and geometries to be evaluated, albeit at slightly reduced data accuracy.

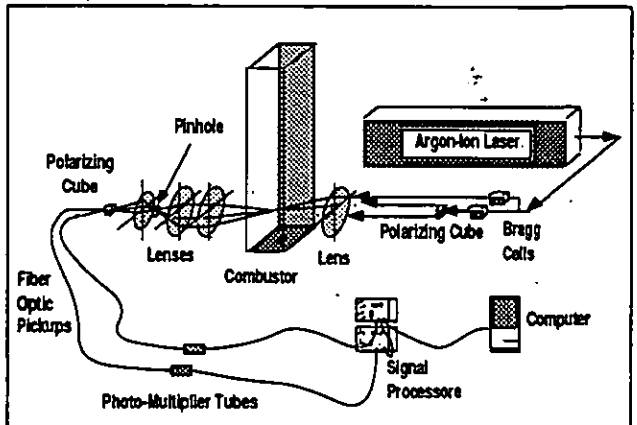

FIGURE 4. SETUP FOR LDA VELOCITY MEASUREMENTS

The two component velocity data (either axial and radial, or axial and tangential) were obtained for each of the test conditions described above (Table 1). The burner was translated with respect to the laser diagnostic volume in an X, Y, and Z coordinate system. Translation in the Z coordinate direction allowed different axial locations to be sampled. Translation in the X or Y axis allowed different radial locations to be sampled. For these tests, the X or Y translations were done along a coordinate centerline. Translation in the X coordinate direction along the Y coordinate centerline allowed axial and radial velocity data to be obtained. The edge of the windows limited translation in this coordinate direction to about ± 30 mm. Translation in the Y coordinate direction along the X coordinate centerline allowed axial and tangential velocity data to be obtained. As the diagnostic volume was brought near the quartz windows, significant optical noise was added to the Doppler signals. The quartz windows were approximately ± 75 mm from the center of the reactor. The optical noise from the windows generally limited data collection to ± 65 mm, although with especially clean windows, it was sometimes possible to get good data at ± 70 mm.

Typically, data was collected at 0.5 or 1.0 mm radial increments where the velocity gradients were large. Data was collected at up to 10 mm increments where velocity profiles were relatively flat. A typical set of data was taken at axial locations of 10, 15, 20, 25, 50, 75, 100, 125, 150, 200, and 240 mm above the dome of the reactor. Occasionally, other intermediate locations were examined where large velocity gradients or other interesting behavior were found.

The basic flow field in the combustor was derived by interpolation of the velocity data obtained. The field is dominated by multiple regions of flow recirculation. The axial velocity from both the X and Y coordinate traverses has been combined for one of the Task 150-HS cold flow cases (14 slpm N_2, 500 slpm air), interpolated, and the zero axial velocity contours plotted in Figure 5. Each zero axial velocity contour bisects a recirculation zone. While the data have not been

analyzed in the detail needed to totally quantify the recirculation patterns, estimates of the recirculation zones are indicated. Eventually, flow streamlines will be plotted to better identify the various flow fields. However, for this paper, only axial, tangential, or radial data have been used.

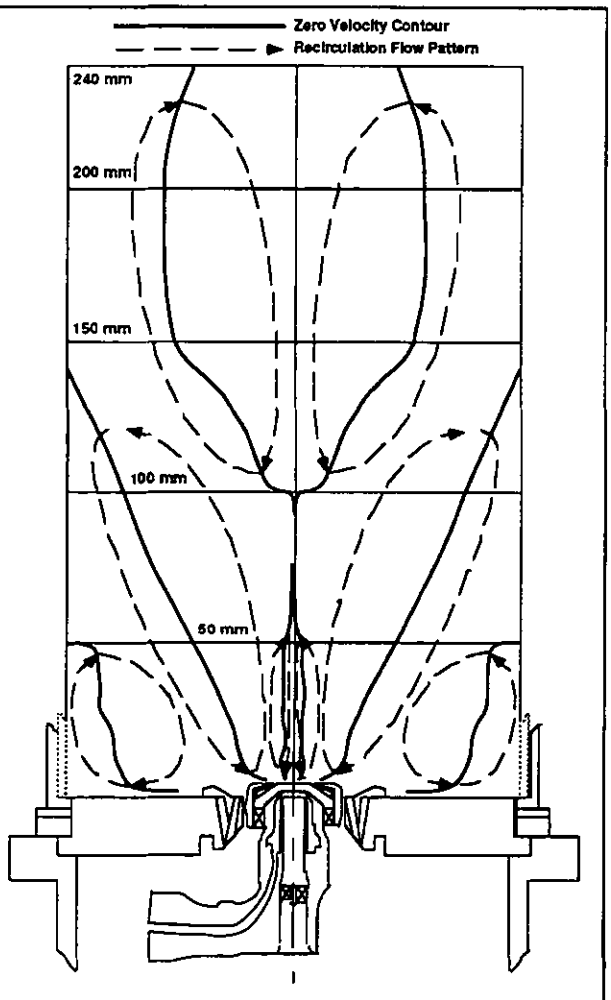

FIGURE 5. RECIRCULATION PATTERNS WITH THE HIGH-SWIRL FUEL INJECTOR

Figure 5 identifies several important recirculation zones. Although the near-field is similar to that in a real gas turbine combustor, the downstream region in not due to the absence of air addition by means of transverse jets, as is usual practice. Since current interest is concentrated on the near-field, this deviation is not of great significance. It is interesting to note that there is a zone of flow reversal on the centerline of the burner very near the discharge of the injector. This flow reversal is undoubtedly caused by the highly swirling flow, and is consistent with the strong vortex structures observed earlier (Figure 3). A recirculation zone is also apparent in the lower corners of the combustion chamber. This zone appears to be driven by the dome cooling jets, and is consistent with the observed horizontal flow in the radial direction that emanates from these cooling jets.

Another major recirculation zone is centered on the zero axial contour that angles from the face of the injector outward till it reaches the wall of the combustor at a down stream location at about 140 mm. This large recirculation zone seems to have a major impact in stabilizing the flame under certain operating conditions. The last observed recirculation zone surrounds the zero iso-velocity contours that exist between the 100 mm and 240 mm axial locations. This recirculation pattern was very weak as judged by the magnitude of the velocities measured, and was only observed in the isothermal case. It was not seen in the combusting cases. The influence of the combustion was sufficient to eliminate this pattern from the flow field. Combustion also altered the shape and location of the other recirculation zones, but each of the other zones remained in the combustion cases.

Figure 6A, 6B, and 6C present the iso-contour plots for the mean axial, mean tangential, and mean radial velocity measurements respectively for the fuel lean case ($\phi = 0.72$). In each figure, the velocity contour plot from the centerline to the maximum measurement radius was created using commercial computer software, duplicated, and reversed. The reversed image was combined with the original image and superimposed on a schematic of the burner to provide an indication of the flow characteristics with respect to the burner. The data presented in Figure 6A and 6B were collected along the Y coordinate direction out to about 60 mm. The data in Figure 6C are limited to a radial location of about 30 mm because of the width constraints of the windows. The flow fields and recirculation patterns presented here are generally consistent with those observed in Figure 5.

The flame at this operating condition was well attached to the center of the injector, and was considered to be fully developed as was shown earlier in the discussion of Figure 3. Mass balance calculations based on isothermal axial velocity measurements have been used to determine the overall accuracy of the LDA measurements. It was found that the mass flow rate was strongly influenced by the gradient assumed near the wall, but reasonable velocity interpolations gave reasonable mass balance closure.

The sharp peak in axial velocity component shown in Figure 6A near the injector is clearly evident. The rapid decay of the high velocity region near the injector as one moves down stream is also apparent. The recirculation zone directly over the injector is dramatic, and clearly shows a significant region of flow reversal. The tangential velocity in this zone is very high as seen in Figure 6B. The other major recirculation pattern in the combustor is of a somewhat different shape and in a somewhat different location than observed in the isothermal case (Figure 5). The recirculation patterns caused by the dome jets are notably absent. Visual observations confirmed that the corner recirculation still existed in the combustion flow cases, but it was not possible to collect LDA data close to the window near the bottom of the reactor because of excess optical noise.

The radial velocity data are presented in Figure 6C. These data are limited to a radial location of about 30 mm. The radial flow velocities are all very low in magnitude, but do showsomeinteresting structures. The low magnitudes of these velocities are close to the resolution of the LDA instrument A similar set of gas velocity data for the Task 150-HS combustor operating at a fuel equivalence ratio of 1.49 is presented in Figures 7A, 7B, and 7C for the mean axial, mean

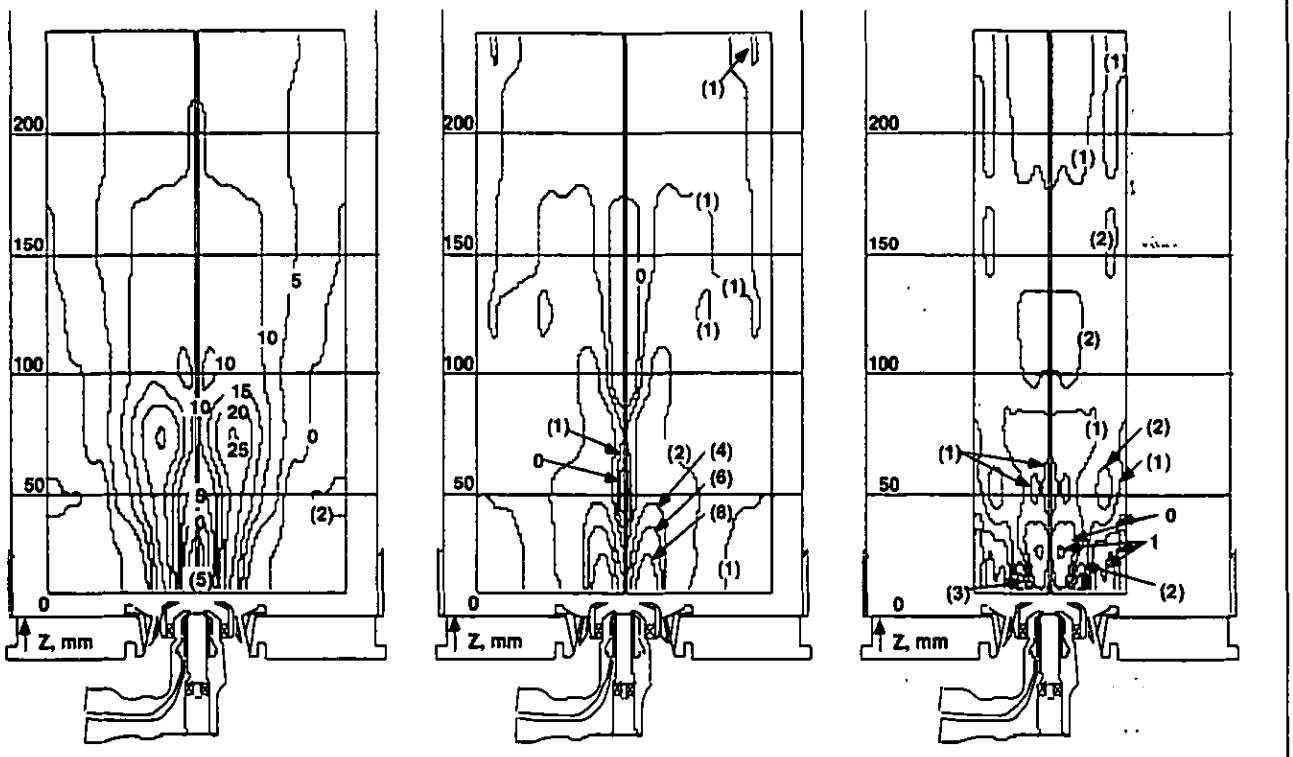

FIGURE 6. ISO-VELOCITY CONTOURS FOR THE T150-HS BURNER AT ϕ = 0.72 AND 500 SLPM AIR FLOW RATE

tangential, and mean radial velocity measurements, respectively. The flame at this operating condition was attached to the insert and dome jets as was shown earlier in the discussion of Figure 3. As above, the radial data in Figure 7C are limited to a radial location of about 30 mm, but the axial and tangential data in Figures 7A and 7B were collected out to about 60 mm. The flow fields and recirculation patterns presented here are also generally consistent with those observed in Figures 5 and 6.

As for the $\phi = 0.72$ case, the sharp peaks in mean axial velocity component associated with the injector are still clearly evident, but seem to decay more rapidly than in the $\phi = 0.72$ case. The recirculation zone directly over the injector is still dramatic, and shows little difference in the magnitude of the reversed velocity or in the size and shape of the recirculation pattern when compared to the $\phi = 0.72$ case. The other major recirculation pattern in the combustor is of a similar shape to that observed with the $\phi = 0.72$ case, but seems to be much stronger (i.e. has much larger reversed flow velocity components). The recirculation patterns caused by the dome jets are still absent. As in the $\phi = 0.72$ case, visual observations confirmed that the corner recirculation still existed in this combustion flow case, but it was not possible to collect LDA close to the window near the bottom of the reactor because of optical noise near the quartz windows.

The radial velocity data are presented in Figure 7C. Again, the radial flow velocities are all very low in magnitude, but do show some interesting structures, that are quite different than seen with the lean flame. The low magnitudes of these velocities are also close to the resolution of the LDA instrument.

The differences in velocities between the lean flame and the rich flame show that there is a strong influence of the location of the flame zone on the flow fields as characterized by the measured velocity fields.

GAS TEMPERATURE MEASUREMENTS

Coherent anti-Stokes Raman spectroscopy (CARS) was used to obtain a set of gas temperature measurements in the Task 150-HS combustor at fuel equivalence ratios of 0.75, 1.00, 1.25, and 1.50; and at an air flow rate of 500 slpm. The details of the CARS facility has been well documented in previous publications (Boyack and Hedman, 1990; Hancock et al., 1991, 1992). The CARS setup used for this study, as shown inFigure 8, is very similar to the folded box-CARS phase matching scheme employed by Boyack (Boyack and Hedman, 1990). Boyack located his combustor directly on the CARS optical table, and was able to easily focus the laser beams

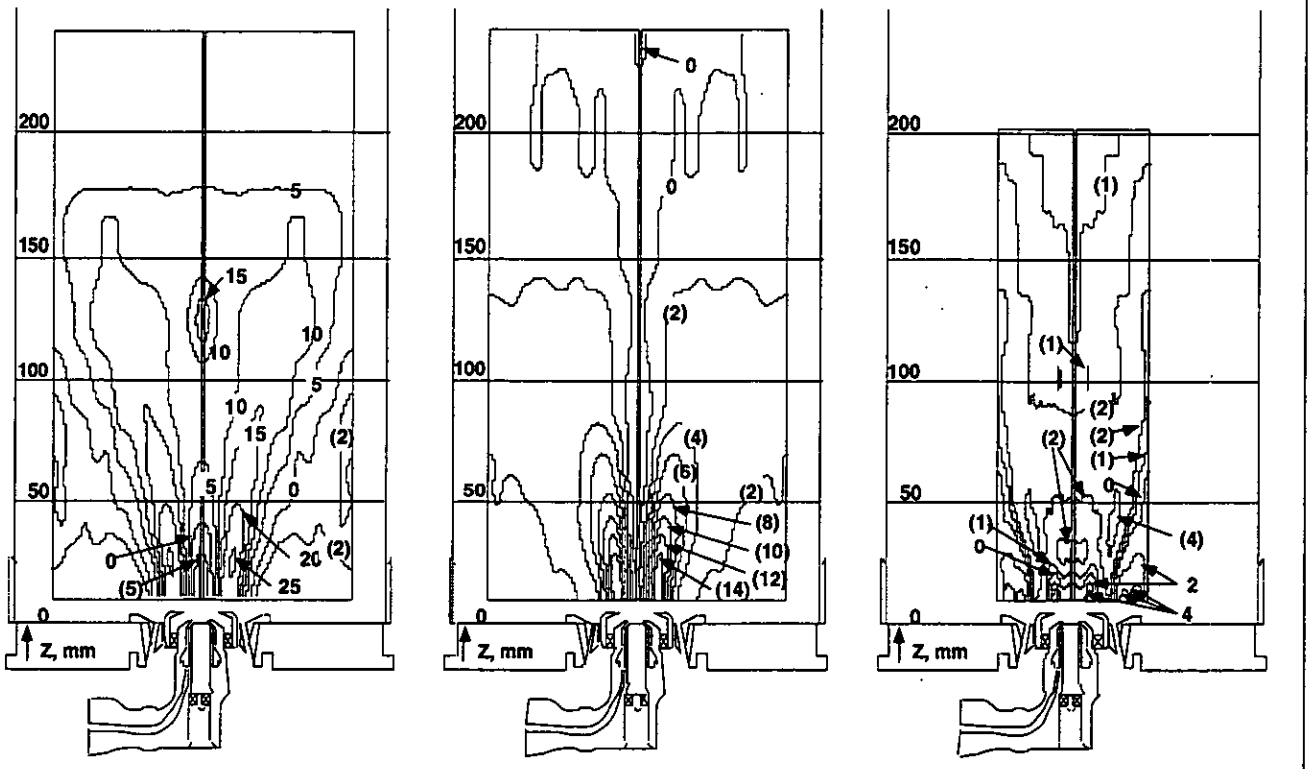

FIGURE 7. ISO-VELOCITY CONTOURS FOR THE T150-HS BURNER AT ϕ = 1.49 AND 500 SLPM AIR FLOW RATE

directly into his combustor. In this experimental setup, the combustor was remotely located. Consequently, the laser beams were directed off the optics table over a distance of about 10 m onto a set of optical bread boards located on either side of the Task 150-HS combustor. The optical components needed to create the box-CARS phase matching were located on these remote optical breadboards. As with Boyack's work, the CARS signal was focused into the end of the fiber optic used to transfer the signal back to the spectrometer. The CARS lasers and spectrometer were keep in an optics room distant from the combustion facilities in an effort to keep the optical components relatively clean.

Like the gas velocity measurements, the CARS temperature measurements were taken at closely spaced radial increments where large gradients in temperature were found and in a courser grid where the temperature gradients were found to be relatively shallow. Temperature data was take at similar axial locations as well. The temperature data were taken along the X coordinate, and consequently are available only out to a radius of about 30 mm, but were taken to an axial location of about 300 mm. Attempts at obtaining data along the Y axis to radial locations near the quartz window resulted in laser damage to the quartz window. Nevertheless, the CARS temperature data obtained have provided adequate temperature measurements to well quantify the temperatures in the region of most interest near the injector.

Figure 9 presents an iso-contour plots of temperature data for the Task 150-HS combustor operating with an air flow rate of 500 slpm and at fuel equivalence ratios of 0.75, 1.00, and 1.50. The data at ϕ =1.25 have been excluded from the paper because of space considerations. Two hundred discrete temperature data points were taken at each of 92 separate diagnostic locations from the centerline to a 30 mm radial location, and from 10 mm to 300 mm axial location. These sets of data were used to determine the mean temperatures used to create the iso-thermal contour plots shown. In order to show the symmetry of the flame, the contour plot was duplicated, and computer software was used to flip the image and add it to the opposite side of the combustor. The flow fields are very symmetric about the centerline in this highly swirled flame. The doubled image gives a better representation of the temperature field in the vicinity of the injector.

The relatively cold region (600 K to 1000 K) directly above the injector in all three cases generally corresponds the central recirculation zone seen in the gas velocity plots (Figures 6 and 7). Surrounding the cold central zone is an intermediate temperature region that seems to be associated with thepenetration of the very high axial velocity into thecombustor. Higher temperatures exist on either side of this penetration zone. It is unfortunate that temperature data could not be obtained in the lower comers of the combustor where

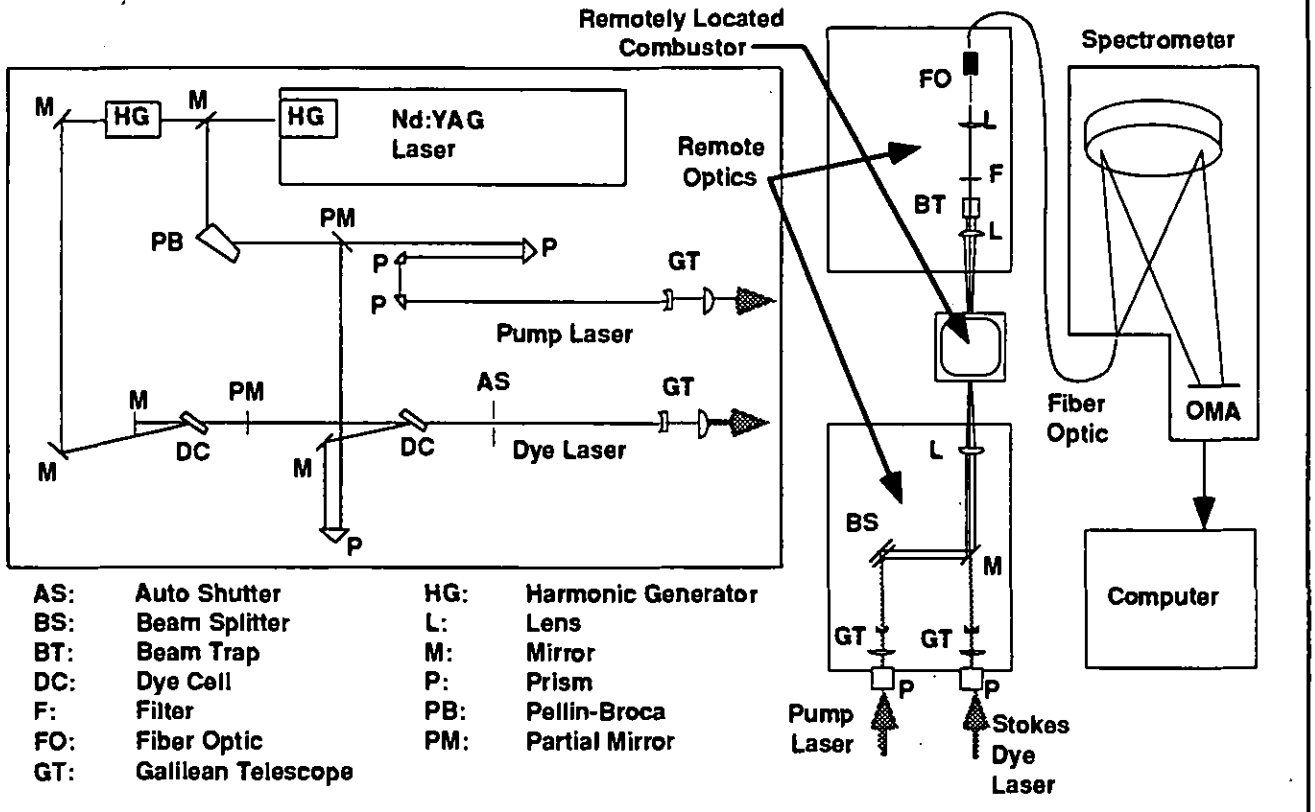

FIGURE 8. SCHEMATIC OF CARS SYSTEM INSTALLATION ON THE COMBUSTOR

the recirculation zones near the dome are located. The data do suggest that this region is relatively cool for the $\phi = 0.75$ case, but seem to indicate a relatively hot region in this corner recirculation zone for the $\phi = 1.5$ case. This observation seems to be consistent with the observed relocation of the flame zone from the central core of the vortex when operating fuel lean to the outer recirculation zone when operating fuel rich, as noted in the digitized film images and in the PLIF images of OH radical discussed in the last section of this paper.

Temperatures in excess of the $\phi = 0.75$ adiabatic flame temperature (1963 K) are seen in a zone near the centerline at an axial location of about 100 mm for the fuel lean case. Since this is a non-premixed flame, this suggests that this diffusion zone may be operating with near stoichiometric ($\phi = 1.00$) mixtures of fuel and air. The peak temperature that was measured was 2085 K which is about 178 K below the theoretical stoichiometric adiabatic flame temperature of 2263 K.

In the stoichiometric case ($\phi = 1.00$), the peak measured temperature is 67 K below the theoretical stoichiometric adiabatic flame temperature of 2263 K. The zone of near peak temperature extends from an axial location of about 100 mm to about 170 mm and forms a toroidal shaped ring around the centerline. Beyond the high temperature region, the temperatures decrease, dropping to about 1800 K at the combustor exit (not shown).

Iso-contour plots of gas temperature measurements for the $\phi = 1.50$ case are shown in Figure 9C. It is interesting to note that the peak temperature (1875 K) in the fuel rich case, like the stoichiometric case, is just below the predicted ($\phi = 1.50$) adiabatic flame temperature of 1974 K It seems reasonable that the peak measured temperature in this case would be close to the adiabatic flame temperature, since all of the oxygen would be consumed early in the flame preventing a zone near stoichiometric to ever exist.

The variation in temperature field as the fuel equivalence ratio changes from fuel lean to fuel rich seems to be consistent with the observations made from the still photographs. At $\phi = 0.75$, the flame is well attached to the burner, with a narrow vortex penetrating into the injector and a fully developed flame structure attached to the injector. The temperature distributions at $\phi = 1.0$ and $\phi = 1.25$ (not shown) were very similar, and seemed to agree with the flame structures described in Figure 3 as a rich lifted flame and a funnel shaped flame. At $\phi = 1.50$ (Figure 9C), the center cold zone has been reduced in size, and there are higher temperatures at the outer edge of the measurement region that support the visual observation that the flame is attached to the insert jets.These results also suggest that a fairly high temperature exists in the corner recirculation zone when the combustor is operating in a fuel rich mode. In general, the temperature measurements are consistent with the visual flame conditions,

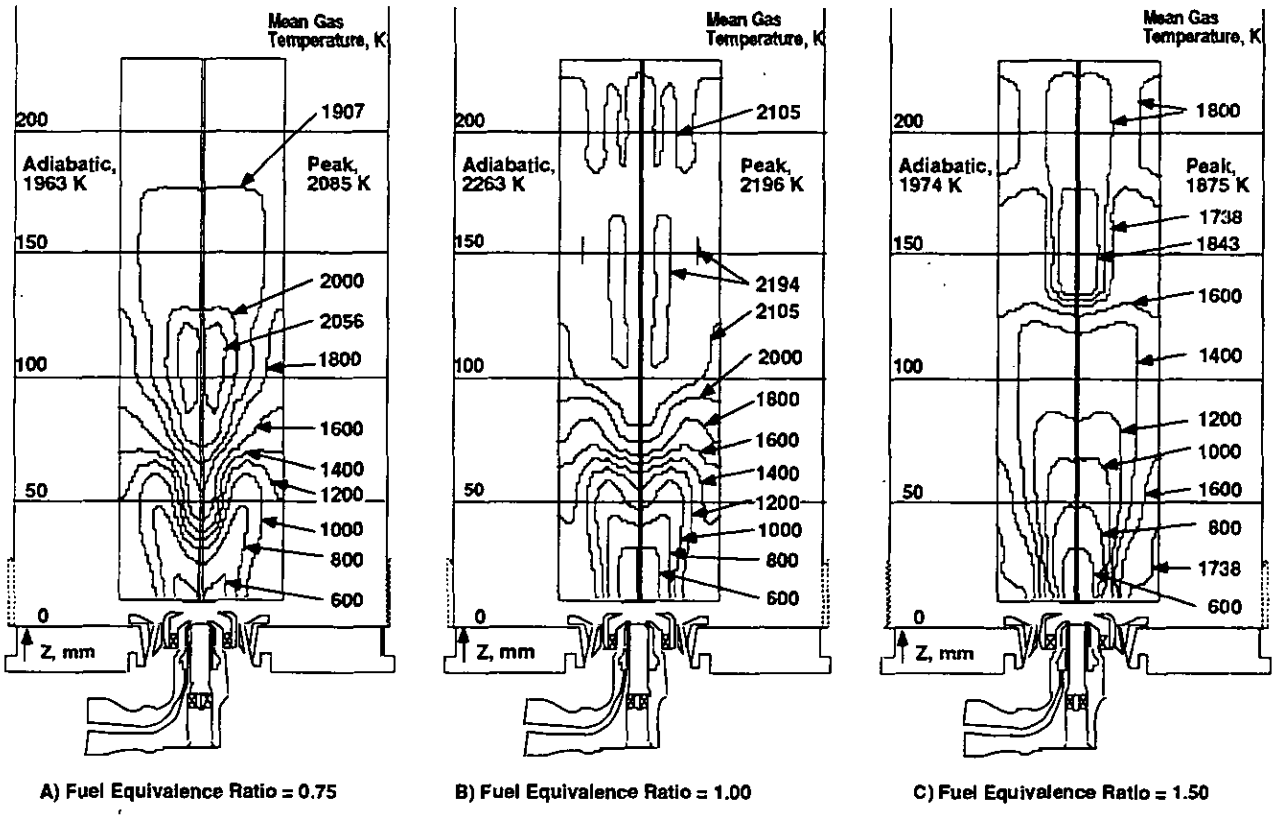

A) Fuel Equivalence Ratio = 0.75 B) Fuel Equivalence Ratio = 1.00 C) Fuel Equivalence Ratio = 1.50

FIGURE 9. MEAN GAS TEMPERATURE ISO-CONTOURS FOR THE T150-HS BURNER AT 500 SLPM AIR FLOW RATE

the PLIF images of the OH radical, and the velocity measurements for this particular test condition.

PLIF IMAGING OF OH RADICAL

In PLIF (planner laser induced fluorescence) imaging, a dye laser is tuned to a resonant frequency which causes the particular combustion radical or molecule to fluoresce at a different resonant frequency. This fluorescence is then recorded and the two-dimensional image preserved with an electronic camera. In these experiments, OH radicals were excited with an ultra-violet (ca 283 nm) light sheet produced by a tunable dye laser pumped with a 10 ns pulse from a Nd:Yag laser. This sheet of laser light was passed through centerline of the reactor. An intensified CCD camera, located normal to the laser sheet, captured the 75 mm high two-dimensional uv (ca 308 nm) image (Figure 10). This nearly instantaneous map of OH radical concentration in the flame zone was then stored by a Macintosh computer. The images have been analyzed and enhanced using conventional computer software.

OH radicals are commonly chosen for PLIF because they are important markers in hydrocarbon flames. These radicals are produced in large quantities during the combustion process, and are a good indicator of flame fronts. However, in some circumstances, these radicals may persist for long distances downstream of the actual flame front, limiting their usefulness. Also, as in any laser diagnostic technique, there is a concentration level below which the OH radical will not be detected. With these limitations in mind, conclusions based solely on PLIF images of the OH radical must be carefully drawn.

Many PLIF images of the OH radicals were obtained in the Task 150-HS combustor at 500 slpm air flow and at fuel equivalence ratios that ranged from 0.62 to 1.75. Images were taken at values of fuel equivalence ratio that roughly correspond to the changes in flame structure that had been observed visually and documented with still photographs (Figure 3). Comparison of the two types of flame image, and the relation of these images to the time-mean flow field and bulk equivalence ratios, explains much about the flame structures. However, comparison of a sequence of instantaneous OH images at fixed operating conditions, e.g. Figure 11, also reveals the highly non-stationary character of the flame zone. This behavior is similar to that observed previously in the Task 100 research combustor (Roquemore, et al, 1991).

The experimental behavior of the Task 100 research combustor is quite different than the predictions by computational fluid dynamics (CFD) programs. These computer codes predict the flame to be anchored in the jet shear layer for all fuel equivalence ratios. However, the flame has been experimentally observed (Roquemore, et al. 1991) to attach to the backward facing step just outside the air tube at

fuel equivalence ratios (ϕ) in excess of 1.08. In these operating conditions, a small "coke bottle" shaped flame pilots a thicker flame sheet which is much lower in the combustor than the CFD programs predict. A waisting in the flow field is predicted by the CFD code, but the mixture is predicted to be too lean to burn. Roquemore postulates that a discrete and intermittent process is responsible for the entrainment of the fuel into the step recirculation zone. This type of transport would require passageways in the flame in order to deliver the unburned fuel from the fuel tube to the step recirculation zone. These passageways would appear as a region with little to no OH radical present.

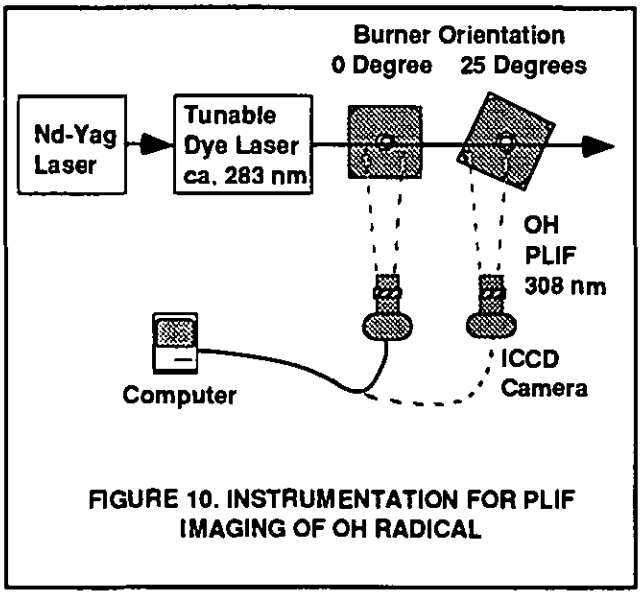

FIGURE 10. INSTRUMENTATION FOR PLIF IMAGING OF OH RADICAL

Much of what Roquemore postulated has been found in PLIF images of the OH radical collected in the Task 100 research combustor. In the well-attached flame (ϕ=1.56), the OH radicals appear in vortex structures being shed off the backwards step. These structures were very clear in the images collected. In the lean condition, OH radicals were not observed below 150 mm in the reactor, with relatively small amounts between 150-200 mm and very large amounts beyond. Similar observations have been made in the PLIF images of the OH radical for the Task 150 technology combustor (e.g. Figure 11 and Figures 12A, 12B, and 12C). Figure 11 shows four separate instantaneous images at two different axial locations at ϕ = 1.29. Figure 12 shows composites of several single PLIF images of OH radical grouped as a collage in the appropriate locations within the combustor at a fuel lean condition (ϕ = 0.62), near stoichiometric (ϕ = 1.08), and at a fuel rich condition (ϕ = 1.49). These images dramatically illustrate the characteristics of swirling flames and the highly variable nature of the instantaneous flame shape. Therefore, it seems likely that the conclusion reached for the co-axial jet system of the Task 100 research combustor (Roquemore et al., 1991; Sturgess et al., 1992; Sturgess et al., 1991b), that mass transport in axisymmetric, turbulent, recirculating flames is dominated by non-stationary flow phenomena, and not by gradient transport is confirmed, even in a practical injection system. The implication of this finding for accurate mathematical modeling of practical turbulent combustion systems is very important.

It is informative to correlate these OH images with the information known about the partitioning of the air flow rates through the various air passageways through the nozzle. The local fuel equivalence ratios shown in Table 2 were calculated from the air flow through each of the different passageways and the total fuel flow. Implicit in these calculations are two assumptions. First, the fuel is assumed to mix uniformly within each combination of partitions before mixing with remaining air. Second, any fuel blockage effects (which would change the partitioning as a function of fuel flow) are assumed to be negligible. At this air flow rate (500 slpm), LBO occurs at a fuel equivalence ratio of about 0.42.

TABLE 2
LOCAL ϕ FROM TOTAL FUEL FLOW AND AIR FOR EACH FLOW PASSAGE COMBINATION

Overall ϕ	ϕ with air from primary swirler	ϕ with air from primary + secondary swirlers	ϕ with air from primary + secondary swirlers + insert jets
0.62	4.17	1.11	0.80
1.08	7.26	1.94	1.39
1.49	10.02	2.67	1.92

With these assumptions in mind, and knowing the flammability limits (ϕ) of propane are roughly 0.5 to 2.5, some conclusions can be cautiously applied to these images. In every case, the air in the primary swirler alone does not provide sufficient oxidizer to permit combustion. Thus, the fuel must mix with at least the secondary swirled air before combustion is possible. As shown in Figure 12A, with a fuel equivalence ratio of 0.62, the funnel structure expected in a swirl stabilized flame is clearly evident. The local fuel equivalence ratio with the air from the two swirled jets is 1.11, indicating little air from the insert jets is needed to complete the combustion. Although Figure 12A shows high concentrations of OH radical extending above the funnel like structure, visual observations reveal the visible flame region is apparently only a thin sheet, much like a horn, or funnel, with a rounded cusp.

As the overall fuel equivalence ratio is increased to 1.08 (Figure 12B), the swirled air/fuel mixture was still within flammability limits. What changed was the extra fuel left to mix with the insert jets. This additional fuel, as shown in Figure 12B, apparently burned on the shoulders of the funnel like structure. Finally, as the overall fuel equivalence ratio is increased to 1.49 (Figure 12C), the very fuel-rich swirled air directly over the injector can no longer support combustion. The estimated fuel equivalence ratio in this central zone is estimated to be about 2.67 which exceeds the rich flammability limits for propane and air. The characteristic funnel of a swirl stabilized flame is no longer visible in Figure 12C. The combustion is only taking place where air from the insert and dome jets has reduced the local fuel equivalence ratio to within the flammability limits of propane and air. This can

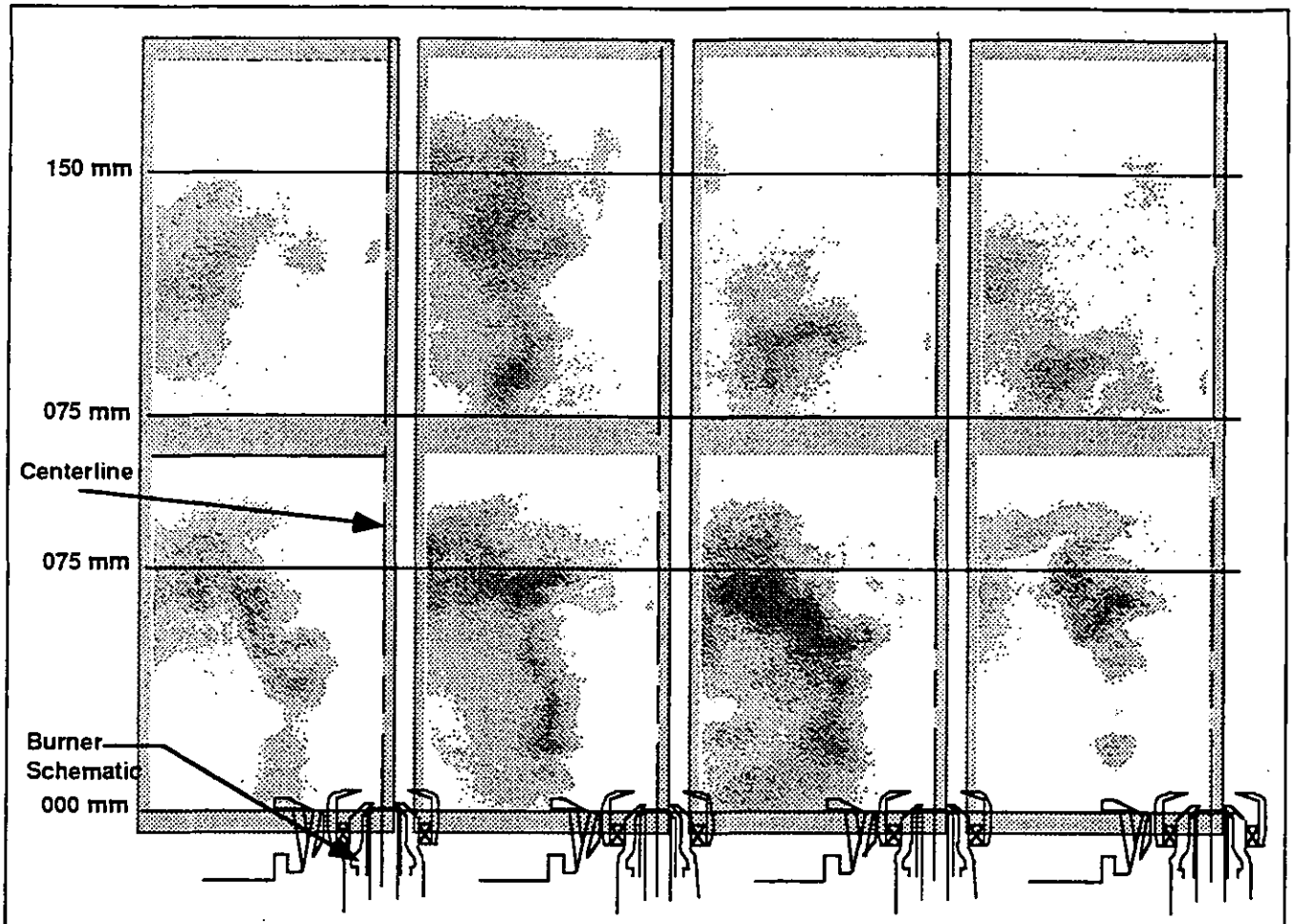

FIGURE 11. INSTANTANEOUS FLAME IMAGES BY PLIF OF THE OH RADICAL (T150-HS NOZZLE, 500 SLPM AIR, PHI 1.29)

be illustrated by comparing Figure 12A with Figure 12C. These two images appear to be negatives of each other--where one is black the other is white. This tends to support an assumption of the fuel mixing with each air passageway in turn from the inside-out.

OBSERVATIONS AND CONCLUSIONS

There have been considerable insights into the operational characteristics of a practical injector gained from this study. However, there is much to be done before a full understanding of the combustion characteristics of a practical gas turbine combustor is achieved.

A complex series of intricate flame shapes have been observed in the Task 150 technology combustor. Each flame shape indicates a different mode of operation, which differ from one another in the location of the flame fronts, or by some structure such as thickness or intensity. The different structures observed arise from changes in the flow fields, mixing patterns, or fuel equivalence ratio as operating conditions are varied. The fuel equivalence ratio where the flame transitions from one structure to another is the major operating variable affecting flame structure. The flames were attached to the insert air jets when the burner was operated very fuel rich. The flame would then lift, reattach, and lift again as the fuel equivalence ratio was progressively reduced. During the reattachment phase, the flame would take on many of the characteristics of a strong vortex and showed characteristics much like a tornado. Consequently, the terminology of funnel cloud, tornado, and debris cloud were adopted to describe some of the observed flame structure.

Gas velocity measurements were made where the flame is well attached to the injector ($\phi = 0.72$), at fuel rich conditions ($\phi = 1.49$) where the flame is attached to the dome and insert jets, and in isothermal, non-reactive flows where nitrogen was substituted for the propane fuel. These velocity data have allowed the effect of the flame temperature on the flow field and gas velocities to be determined.

Gas velocity data near the injector have shown sharp peaks in mean axial velocity near the outlet of the injector, and a corresponding strong tangential component in this same location. The insert jets had a marked influence on the axial and radial components, but seemed to have little effect on the tangential velocity components. The sharp gradients in axial velocity component were observed to decay quite rapidly with

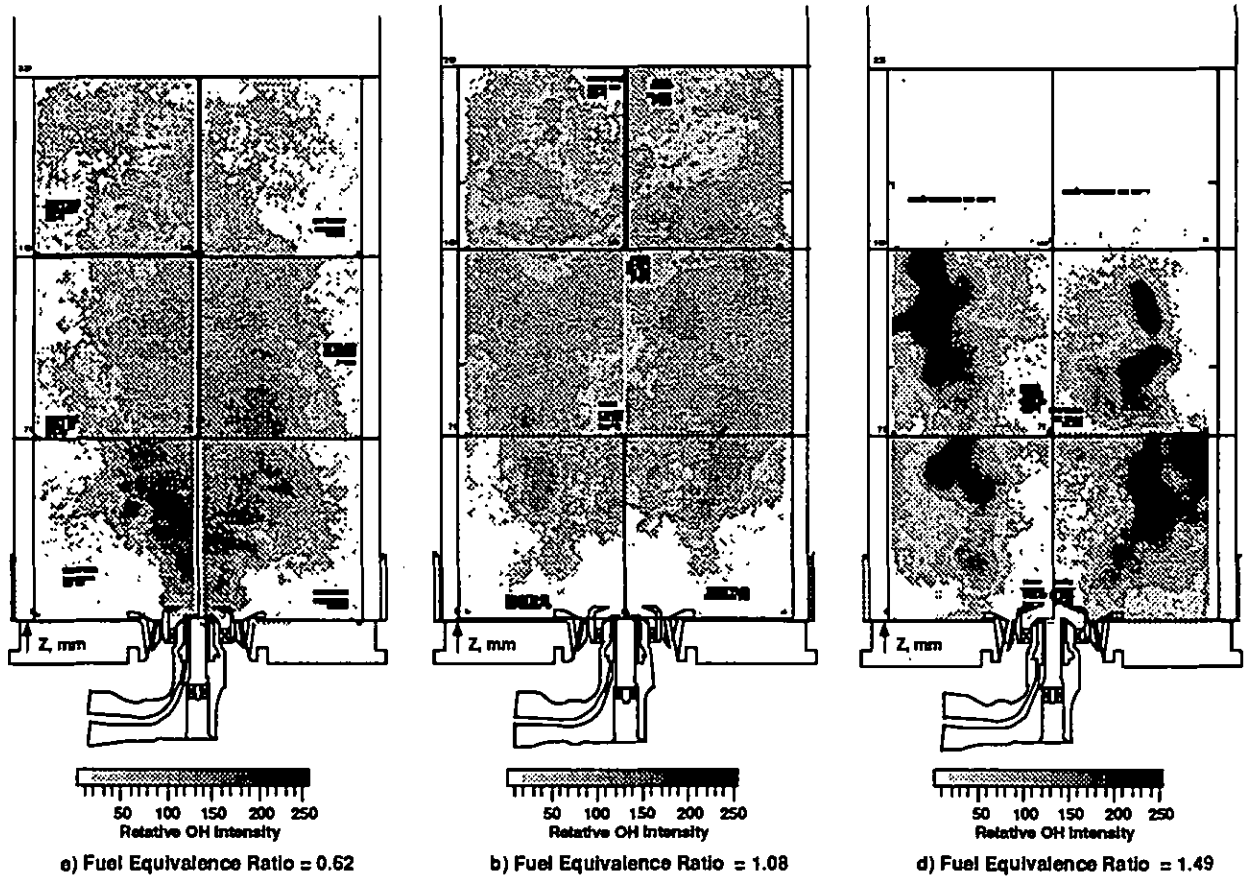

FIGURE 12. INSTANTANEOUS PLIF CONTOURS OF OH RADICAL (T150-HS BURNER, 500 SLPM AIR)

increasing downstream position. The strong tangential velocities associated with the injector rapidly decayed and diffused to the outer edges of the reactor becoming nearly uniform (ca -1 m/s) across the duct by the 150 mm axial location. Mass balance calculations based on isothermal axial velocity measurements have been used to determine the accuracy of the LDA measurements, and to assist in the extrapolation of the velocity to the wall. The mass flow rate is strongly influenced by the gradient assumed near the wall, but reasonable velocity interpolations gave reasonable mass balance closure.

Images from still photographs and angular velocity data deduced from the tangential velocity measurements have shown that the flow in the region behaves much like that observed in a strong vortex, with the rotational speed in rpm increasing towards infinity as the zero radius position is approached. The high rotational speeds are consistent with visual observations of the flames. The steep gradients in angular velocity suggest the shear stresses in the swirling eddies are very high.

An analysis of the zero axial velocity contours for one of the iso-thermal flow cases (14 slpm N_2, and 500 slpm air) has been used to show the complex flow structure that includes four recirculation zones: one at the bottom edge of the reactor driven by the dome jets., a second small but intense recirculation zone associated with the injector swirlers directly over the injector, a third major recirculation zone that begins at the edge of the injector and angles upward to the wall of the reactor, and a weak fourth recirculation zone high up in the combustor. The weak fourth zone was not seen in the combusting flows. The recirculation zones are consistent with the visual observations and video images taken of the reactor.

CARS gas temperature measurements have been successfully made in the Task 150 technology combustor. The measured peak temperatures were slightly below the predicted adiabatic flame temperature for the stoichiometric and fuel rich cases. The peak temperature was slightly higher than the adiabatic flame temperature for the lean case, which suggests a local diffusion zone within the flame that is close to a stoichiometric fuel equivalence ratio.

The variation in temperature field as the fuel equivalence ratio changes from fuel lean to fuel rich seemed to be consistent with the observations made from the still photographs. In general, the temperature measurements are consistent with the visual flame conditions, the PLIF images of the OH radical, and the velocity measurements for this particular test condition.

The PLIF images of the OH radical taken with the Task 150-HS technology burner dramatically illustrate the characteristics of swirling flames and the highly variable nature of the flame shape. The air from the insert jets significantly affects the flame structure, and the different modes of operation observed. Correlation of these OH images with the partitioning of the air flow rates through the various air passageways of the injector showed a consistent correlation between the local fuel equivalence ratio and the location of the flame structure. The images at low overall fuel equivalence ratio where the flame is well attached to the burner, and the images at high overall fuel equivalence ratio where the flame is attached to the insert jets are negatives of each other--where one is black the other is white. This supports the assumption of the fuel mixing with each passageway in turn from the inside-out.

ACKNOWLEDGMENTS

This paper presents results from an Air Force Office of Scientific Research (AFOSR) program being conducted at Brigham Young University (BYU), Provo, Utah and at Wright-Patterson Air Force Base (WPAFB). This study is part of an extensive research effort being carried out by the Fuels Combustion Group of the Aero Propulsion and Power Laboratory at Wright- Patterson Air Force Base (APPL, WPAFB), Dayton, Ohio, in which simple and complex diffusion flames are being studied to better understand the fundamentals of gas turbine combustion. The program's long term goal is to improve the design methodology of gas turbine combustors.

REFERENCES

Boyack, K.W., and Hedman, P.O., (1990), "Dual-Stokes CARS System for Simultaneous Measurement of Temperature and Multiple Species in Turbulent Flames," Twenty-third Symposium (International) on Combustion, The Combustion Institute, Pittsburgh, PA

Hancock, R.D., Hedman, P.O., and Kramer, S.K., (1991), "Coherent Anti-Stokes Raman Spectroscopy (CARS) Temperature and Species Concentration Measurements in Coal-Seeded Flames," Combustion and Flame, Vol. 71, pp 593-604

Hancock, R.D., Boyack, K.W., and Hedman, P.O., (1992), "Coherent Anti-Stokes Raman Spectroscopy (CARS) in Pulverized Coal Flames," Advances in Coal Spectroscopy, pg 373-407, ed by Henk L.C. Meuzelaar, Plenum Publishing Company

Roquemore, W.M., Reddy, V.K., Hedman, P.O., Post, M.E., Chen, T.H., Goss, L.P., Trump, D., Vilimpoc, V., and Sturgess, G.J., (January 7-10, 1991), "Experimental and Theoretical Studies in a Gas-Fueled Research Combustor," Paper No. AIAA 91-0639, 29th Aerospace Sciences Meeting, Reno, Nevada

Sturgess, G.J., Heneghan, S.P., Vangsness, M.D., Ballal, D.R., and Lesmerises, A.L., (June 3-6, 1991a), "Lean Blowout in a Research Combustor at Simulated Low Pressures," ASME Paper No. 91-GT-359, International Gas Turbine Congress and Exposition, Orlando, FL

Sturgess, G.J., Sloan, D.G., Roquemore, W.M., Reddy, V.K., A.L. Shouse, D., Lesmerises, A.L., Ballal, D.R., Heneghan, S.P., Vangsness, M.D., and Hedman, P.O., (1991b) "Flame Stability and Lean Blowout - A Research Program Progress Report," Proceedings of the 10th ISABE Conference, Nottingham, England, pp 372-384

Sturgess, G.J., Sloan, D.G., Lesmerises, A.L., Heneghan, S.P., and Ballal, D.R., (1992a), "Design and Development of a Research Combustor for Lean Blowout Studies," ASME Journal of Engineering for Gas Turbines and Power, Vol. 114, pp. 13-19

Sturgess, G.J., Heneghan, S.P., Vangsness, M.D., Ballal, D.R., Lesmerises, A.L., and Shouse, D., (June 1-4, 1992b), "Effects of Back-Pressure in a Lean Blowout Research Combustor," ASME Paper No. 92-GT-81, ASME International Gas Turbine Congress and Exposition, Cologne, Germany

Sturgess, G.J., and Shouse, D., (May 1993), "Lean Blowout Research in a Generic Gas Turbine Combustor with High Optical Access," ASME International Gas Turbine Congress and Exposition, Cincinnati, OH